Development 138, 2499-2509 (2011) doi:10.1242/dev.063032

Tangential migration and proliferation of intermediate progenitors of GABAergic neurons in the mouse telencephalon

Shengxi Wu[1,2], Shigeyuki Esumi[1], Keisuke Watanabe[1], Jing Chen[2], Kouichi C. Nakamura[3], Kazuhiro Nakamura[3], Kouhei Kometani[4], Nagahiro Minato[4], Yuchio Yanagawa[5], Kaori Akashi[6], Kenji Sakimura[6], Takeshi Kaneko[3] and Nobuaki Tamamaki[1]

SUMMARY

In the embryonic neocortex, neuronal precursors are generated in the ventricular zone (VZ) and accumulate in the cortical plate. Recently, the subventricular zone (SVZ) of the embryonic neocortex was recognized as an additional neurogenic site for both principal excitatory neurons and GABAergic inhibitory neurons. To gain insight into the neurogenesis of GABAergic neurons in the SVZ, we investigated the characteristics of intermediate progenitors of GABAergic neurons (IPGNs) in mouse neocortex by immunohistochemistry, immunocytochemistry, single-cell RT-PCR and single-cell array analysis. IPGNs were identified by their expression of some neuronal and cell cycle markers. Moreover, we investigated the origins of the neocortical IPGNs by Cre-loxP fate mapping in transgenic mice and the transduction of part of the telencephalic VZ by Cre-reporter plasmids, and found them in the medial and lateral ganglionic eminence. Therefore, they must migrate tangentially within the telencephalon to reach the neocortex. Cell-lineage analysis by simple-retrovirus transduction revealed that the neocortical IPGNs self-renew and give rise to a small number of neocortical GABAergic neurons and to a large number of granule and periglomerular cells in the olfactory bulb. IPGNs are maintained in the neocortex and may act as progenitors for adult neurogenesis.

KEY WORDS: GABA, Adult neurogenesis, Intermediate progenitor, Migration, Neocortex, Neurogenesis, Mouse

INTRODUCTION

In the embryonic neocortex, neuronal precursors are generated in the ventricular zone (VZ) (Kriegstein and Alvarez-Buylla, 2009; Noctor et al., 2001; Miyata et al., 2001; Tamamaki et al., 2001). As the neocortex grows, the neurogenic intermediate progenitors (nIPs) (Kriegstein and Alvarez-Buylla, 2009) of principal excitatory neurons (Noctor et al., 2004; Miyata et al., 2004; Haubensak et al., 2004; Wu et al., 2005; Hansen et al., 2010) and GABAergic inhibitory neurons (Letinic et al., 2002; Inta et al., 2008) appear in the subventricular zone (SVZ). Unlike the neural precursors of the VZ, the nIPs are multipolar as well as bipolar, and they are not fixed to a given position as are, for example, radial glia, which are anchored by their radial processes. Therefore, nIPs may be able to migrate within the neocortex and the telencephalon (Tabata et al., 2009).

The nIPs of the principal excitatory neurons are characterized by their expression of proneural transcriptional factors, such as Ngn2 (Neurog2 – Mouse Genome Informatics) (Miyata et al., 2004), Nex/Math2/Neurod6 (Wu et al., 2005) and Tbr2 (Eomes – Mouse Genome Informatics) (Englund et al., 2005); i.e. they express some markers that are often used to identify neuronal precursors, yet they continue to proliferate. By contrast, the intermediate progenitors of GABAergic neurons (IPGNs) have been identified as proliferating cells, which are positive for Mash1/Ascl1 immunoreactivity and can be labeled by GFP driven by a neuron-specific promoter (Letinic et al., 2002; Inta et al., 2008). Most characteristics of IPGNs, including their sites of origin, are still unclear.

Here, we have used the co-expression of the GABA-synthesizing enzyme GAD67 (Gad1 – Mouse Genome Informatics), a very early marker of the GABAergic fate (Yun et al., 2002), and cell-cycle markers to identify IPGNs in the perinatal mouse brain. We then employed a variety of approaches to investigate their gene expression profiles, origin, migration, fat, and possible roles in the mouse neocortex.

MATERIALS AND METHODS

Animals

All mice were treated in accordance with the Regulations for Animal Care of Kumamoto University. To generate the GAD67-knock-in Cre mice, we designed a targeting vector in which the Cre recombinase gene was inserted into the initial methionine site of the *Gad1* gene in frame. A knock-in vector, pGAD67CreTV, contained a 2.9 kb fragment at the 5′ side, a Cre gene just behind the GAD67 translational start, a *Pgk*-neo-p(A) cassette flanked by two Flp recognition target (frt) sites, a 6.8 kb fragment at the 3′ side and a MC1 promoter-driven diphtheria toxin gene (see Fig. S1A in the supplementary material). Linearized pGAD67CreTV was introduced into C57BL/6 mouse ES cells and the G418-resistant clones were picked up. Positive clones were identified by Southern blot hybridization or PCR. The sequence of these primers is provided in Table S1 in the supplementary material. The TVA Cre-

[1]Department of Morphological Neural Science, Graduate School of Medical Sciences, Kumamoto University, Kumamoto 860-8556 Japan. [2]Department of Anatomy and K. K. Leung Brain Research Centre, Fourth Military Medical University, Xi'an 710032, P. R. China. [3]Department of Morphological Brain Science, Graduate School of Medicine, Kyoto University, Kyoto 606-8501, Japan. [4]Department of Immunology and Cell Biology, Graduate School of Biostudies, Kyoto University, Kyoto 606-8501, Japan. [5]Department of Genetic and Behavioral Neuroscience, Graduate School of Medicine, Gunma University, Maebashi 371-8511 Japan and SORST Kawaguchi, Japan. [6]Department of Cellular Neurobiology, Brain Research Institute, Niigata University, Niigata 951-8585, Japan.

*Author for correspondence (tamamaki@kumamoto-u.ac.jp)

Accepted 22 March 2011

reporter TG mouse was generated by the pronuclear injection of linearized DNA containing CApromoter-loxP-stop-loxP-tvA-stop-polyA (see Fig. S2 in the supplementary material). All the embryos were obtained by timed mating as described in the text. The morning after mating was considered embryonic day 0 (E0). The day of birth was E19 or postnatal day 0 (P0).

Immunohistochemistry and immunocytochemistry

Immunohistochemistry and immunocytochemistry were performed as described previously (Tamamaki et al., 2003a; Wu et al., 2005). The antibodies used in this experiment are anti-βIII-tubulin (mouse Tuj1, Babco 1/500), anti-BrdU (mouse, Becton Dickinson, 1/1000; rat, Abcam, 1/1000), anti-Cre (rabbit, Novagen, 1/5000), anti-cyclin D1 (rabbit, Anaspec, 1/200), anti-Dcx (guinea pig, Chemicon, 1/1000), anti-Delta4 (rabbit, Rockland, 20 μg/ml), anti-Dlx2 (rabbit, a gift from Dr J. L. R. Rubenstein, UCSF, CA, USA, 1/200), anti-GABA (rabbit, Sigma, 1/5000), anti-GAD67 (mouse, Chemicon, 1:500), anti-GFAP (rabbit, Dako, 1/2000), anti-GFP [rabbit and guinea pig (Tamamaki et al., 2000)], anti-Ki-67 (mouse, Becton Dickinson B56, 1/50; rabbit, Epitomics, 1/200), anti-Map2 (mouse, Sigma HM2, 1/250-1/500), anti-Mash1/Ascl1 (mouse, PharMingen, 1/500), anti-NCAM (rabbit, Chemicon, 1/200), anti-nestin (mouse, Becton Dickinson, 1/500), anti-Notch3 [goat, Santa Cruz (M-20), 1/50], anti-PCNA (mouse, Novocastra, 1/100), anti-phosphorylated H3 (rabbit, Upstate, 1/1000), anti-Sox2 (rabbit, Chemicon, 1/1000), anti-TVA (rabbit, a kind gift from Dr A. D. Leavitt, UCSF, CA, USA).

Single-cell RT-PCR and single-cell microarray analysis

The methods for single-cell RT-PCR and single-cell microarray analysis have been described previously (Esumi et al., 2008). PCR primers were designed using the GenBank sequence database for each target gene and are listed in Table S1 in the supplementary material. Microarray data are available at Array Express (Experiment name: Gene expression profiles of intermediate progenitors of GABAergic neuron; ArrayExpress accession, E-MTAB-452)

Fluorescence activated cell sorting and immunoblotting

The caudal two-thirds of the neocortex at E18 was dissected (Fig. 1A) and dissociated into single cells. The GAD67-GFP-positive cells were isolated by sorting using FACSVantage (Becton Dickinson). The sorted cells (5×10^4-10^5 cells) were cultured for 2-7 days. The culture medium was Neurobasal medium conditioned with E17-18 embryonic brain tissue, followed by the addition of 5% B27 supplement, 20 ng/ml bFGF, 20 ng/ml EGF and 5 μg/ml BrdU in the presence or absence of arabinosylcytosine (Ara-C) (0.5 μM). For dot-blots, DNA was purified from the cells and applied to a nitrocellulose membrane (5 ng/dot). After denaturing the DNA, the membrane was incubated with an anti-BrdU antibody. The BrdU-immunoreactivity was detected with an ECL kit (Amersham).

Video-microscopy

Coronal brain slices (100 μm) were placed in the conditioned medium used for the cell culture. In some slices, nuclear division was monitored by the red fluorescence of a histone-H2B-mCherry fusion protein (Kanda et al., 1998). The fluorescent images were captured at 5-minute intervals for 8 hours (Wu et al., 2005).

Electroporation of Cre-reporter plasmids

Plasmids, CApromoter(1.7 kb)-loxP-mRFP(0.7 kb)-stop-loxP-GFP(0.7 kb)-stop-poylA(0.6 kb), CApromoter-loxP-mRFP-stop-loxP-FucciGreen(1 kb; MBL, co LTD, Japan)-stop-poylA, CApromoter-loxP-mRFP-stop-loxP-CFP(0.7 kb)-stop-poylA or CApromoter-FucciGreen-stop-poylA (1 μg/μl) were colored with Indian ink and injected into the third ventricle of E14 GAD67-Cre knock-in mouse embryos or E14 Nkx2.1-Cre mouse embryos (Fig. 6A). Next, we placed a needle electrode at one side of the orbit of the eye and the other, flat electrode on the top of the head of the embryo. By passing the electric current (40 V, 5 Hz square wave, 2 seconds) from the orbit to the parietal brain, the DNA was introduced into VZ cells of the third ventricle before the colored DNA solution could seep into the lateral ventricle. Accordingly, one day after the transduction, mRFP red fluorescence was seen almost exclusively in the wall of the third ventricle.

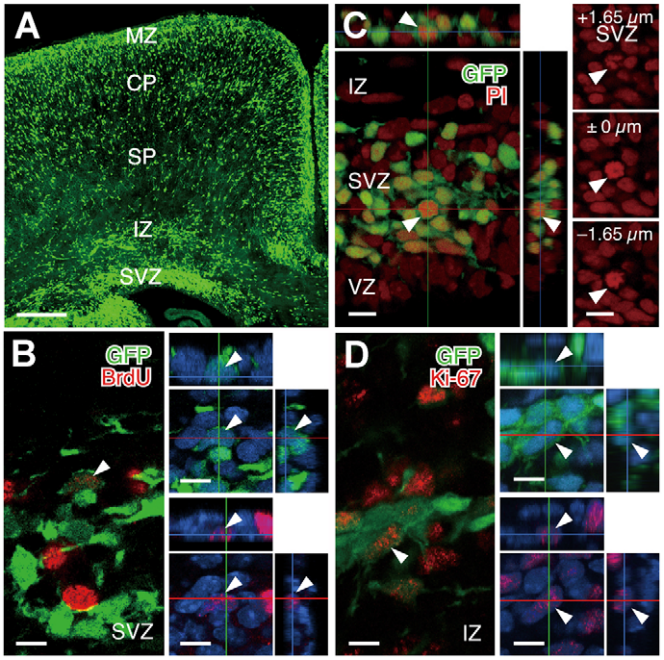

Fig. 1. GFP-positive cells in the GAD67-GFP knock-in mice. (**A**) GFP-positive cells (green) in the neocortex at E18. (**B**) A GFP (green) and BrdU (red) double-positive cell (arrowhead). (**C**) A GFP-positive cell with chromosomal condensation (arrowhead). Insets on the right show the same propidium iodide (PI)-stained nucleus (red) at three different focal planes. (**D**) A GFP (green) and Ki-67 (red) double-positive cell (arrowhead). The right-hand panels in B and D are three-dimensional views of the double-labeled cells. Nuclei in B and D were counterstained with PI (blue in panels at right). CP, cortical plate; IZ, intermediate zone; MZ, marginal zone; SP, subplate; SVZ, subventricular zone. Scale bars: 200 μm in A; 10 μm in B-D.

The labeling was seen occasionally in the medial ganglionic eminence and rarely in the lateral ganglionic eminence. No mRFP fluorescence was seen in the neocortical VZ 1 day after the electroporation. To transduce the neocortical VZ with the GFP Cre-reporter plasmid, we injected the DNA solution into the lateral ventricle, and placed a needle electrode on the surface of the neocortex and the other, flat electrode, on the opposite side of the head of the embryo, at the temporal surface. The current was injected from the needle electrode (n=10). Two or 4 days after the electroporation, the embryos were recovered and fixed in the buffered fixative containing 4% paraformaldehyde, and the head of each embryo was cut into serial sections using a cryostat. The GFP, mRFP, CFP, Fucci-Green and Hoechst fluorescence was observed under a fluorescence microscope. Some sections were autoclaved and processed for immunohistochemistry.

Cre-positive cell-specific transduction with simple retrovirus

RCAS-CMV-GFP recombinant virus was grown in chick embryonic fibroblast cells, harvested and concentrated (1×10^{10}) by sedimentation in an ultracentrifuge (50,000 ***g***). The virus solution was colored with Indian ink. E15-E18 embryos and P0 newborn mice were obtained by mating the TVA Cre-reporter mice and GAD67- or Nkx2.1-Cre-mice. We penetrated the skulls of the embryos caudal to bregma (the frontal suture) with a glass capillary and maintained an angle tangential to the dorsal neocortical surface pointing rostrally. We then injected the virus solution. Four to 7 days later, the mouse brains were recovered, and the infected cells were visualized by GFP immunohistochemistry.

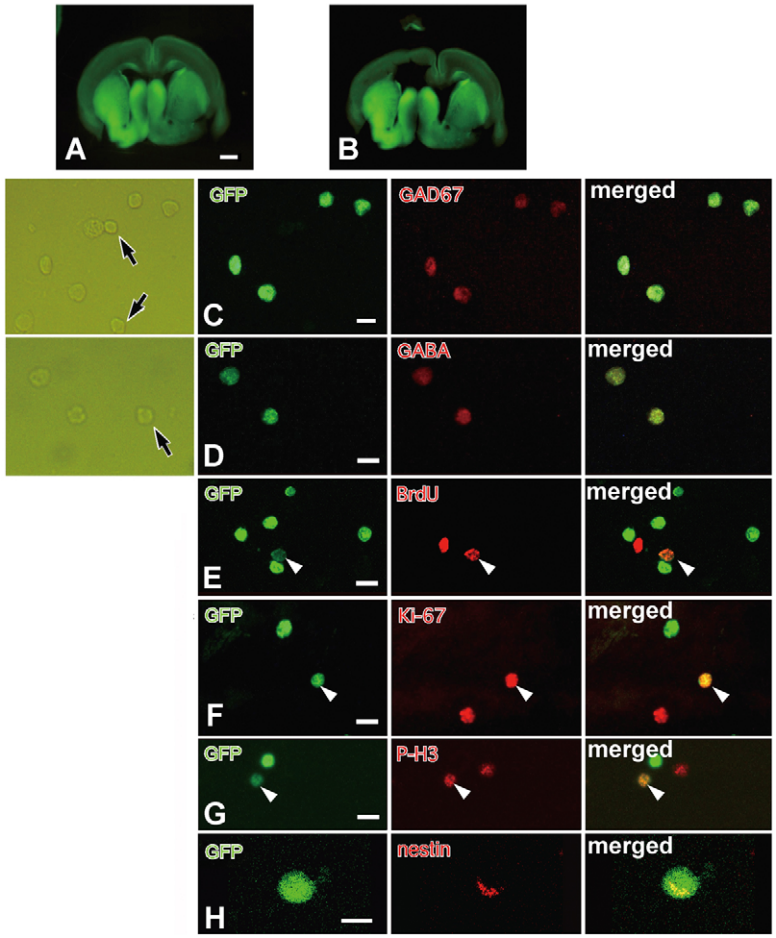

Fig. 2. Immunocytochemistry of dissociated GFP-positive cells. (**A**,**B**) The more ventral regions of the E18 embryonic neocortex (i.e. from the IZ to VZ) of GAD67-GFP knock-in mice were microdissected, dissociated into individual cells and mounted onto glass slides for double-immunostaining for GFP and other markers. (**C-H**) The colocalization of GAD67 immunoreactivity (C), GABA immunoreactivity (D), BrdU immunoreactivity (E), Ki-67 immunoreactivity (F), P-H3 immunoreactivity (G) and nestin immunoreactivity (H) with GFP immunoreactivity. Panels on the left in C and D show bright-field images. Arrows indicate cells negative for GFP immunoreactivity. Arrowheads indicate double-positive cells (E-H). Scale bars: 200 μm in A; 10 μm in C-H.

RESULTS

Colocalization of GAD67 and cell-cycle markers in IPGNs as revealed by immunohistochemistry and immunocytochemistry

GFP-expressing cells in GAD67-GFP knock-in mice (Tamamaki et al., 2003a) were prevalent from the marginal zone (MZ) to the SVZ at E18 in the neocortex (Fig. 1A), and often formed clusters in the SVZ and intermediate zone (IZ). All of them were positive for GABA and GAD67 immunoreactivity (Fig. 2A-D). In addition, the vast majority of the GFP-positive cells in the VZ, SVZ and IZ were positive for MAP2, βIII-tubulin (Tuj1), Dlx2, Dcx and NCAM immunoreactivity (see Fig. S3 in the supplementary material). However, all of the GFP-positive cells in the E18 neocortex are not necessarily positive for these neuronal markers. Some of them may be precursors of GABAergic neurons.

We next used immunohistochemistry and immunocytochemistry to evaluate the colocalization of GFP with cell-cycle indicators. First, we detected cells in the DNA synthetic phase (S phase) using BrdU labeling. Thirty minutes after BrdU injection into the peritoneal cavity of pregnant mice, BrdU immunoreactivity was detected in the E18 mouse neocortex (Fig. 1B, Fig. 2E). (To ease the quantification of GFP/BrdU-double-labeled cells, we counterstained the nuclei with propidium iodide.) The cells that were double-labeled by GFP and BrdU accounted for only 1.5% (4/263 in the IZ and 7/495 in the SVZ) of the GFP-positive cells, but represented 5% of the BrdU-positive cells in the IZ, SVZ and VZ. We also identified GFP-positive cells in mitosis (M phase) in the SVZ by their chromosomal condensation (Fig. 1C).

Immunolabeling for GFP and the proliferation marker Ki-67 (Mki67 – Mouse Genome Informatics) revealed that double-positive cells (Fig. 1D, Fig. 2F) accounted for 22% of the GFP-positive cells in the IZ (75/337) and 29% in the SVZ (96/335) of the dorsal neocortex. Double labeling for GFP and the M-phase marker phosphorylated histone H3 (P-H3; Fig. 2G; see Fig. S4A in the supplementary material) was also seen, starting at E16. In sections immunolabeled for PCNA and GFP, all the nuclei in some clusters of GFP-positive cells were double-labeled (see Fig. S4B in the supplementary material). Some GFP-positive cells were positive for nestin (Fig. 2H). Thus, the cell-cycle markers Ki-67, PCNA, BrdU, P-H3 and a neurogenic marker (nestin) were colocalized with GABA and GAD67 in the GAD67-GFP mice (see Table S2 and Fig. S4B in the supplementary material). To verify that the co-localization of these markers was not unique to the GAD67-GFP knock-in mice, we also immunolabeled the wild-type murine neocortex, and found that the Ki-67 immunoreactivity and GAD67 immunoreactivity were also colocalized in dissociated cells (data not shown). The marker colocalization occurred only after E16.

We also considered whether these co-labeled cells might be neurons in apoptosis, which are known to re-enter the cell cycle, express cell-cycle markers and incorporate BrdU, although they never enter M-phase (Herrup and Yang, 2007). However, chromosomal condensation with P-H3 immunoreactivity is detectable only in M-phase, and, therefore, our immunolabeling results showing these two features indicated that at least some of the GAD67-GFP-positive cells in the neocortex at E18 are IPGNs.

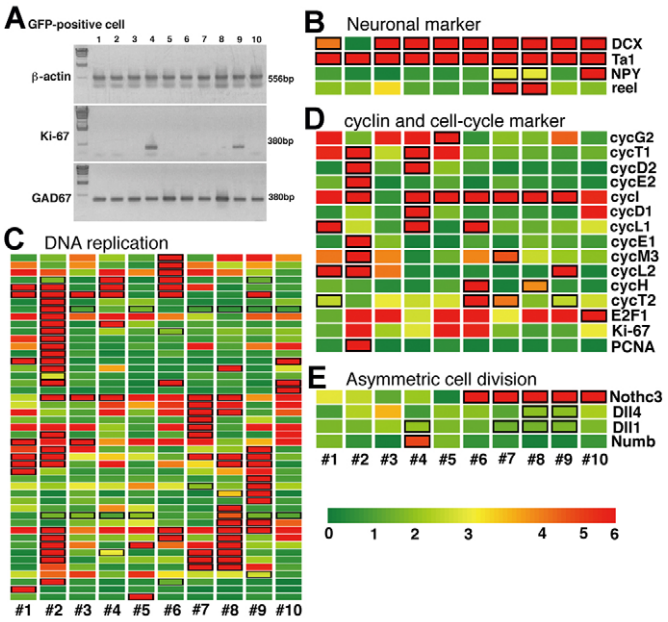

Fig. 3. Gene expression profiles of single GFP-positive cells. (**A**) The expression of β-actin, *Mki67* and *Gad1* was detected by single-cell RT-PCR in 10 GFP-positive cells from the SVZ of the GAD67-GFP mouse neocortex at E18. Two out of the 10 cells co-expressed *Mki67*. (**B-E**) Gene expression profiles of 10 single GFP-positive cells focusing on genes reported to be characteristic of neurons (B); related to DNA replication (C); cyclins, cell-proliferation markers and the cell-cycle suppressor E2f1 (D); and related to asymmetric cell division (E). The common gene names are shown on the right-hand side of panels (B,D,E). The gene names, GenBank accession numbers and gene symbols are listed in Table S3 in the supplementary material. The normalized expression level is indicated by pseudo-colors (from green to red; GeneSpring software). A black rectangle around a colored tile indicates a Present call.

Co-expression of GAD67 and cell-cycle markers in IPGNs as revealed by single-cell gene-expression analysis

To rule out the possibility that our immunolabeling experiments were detecting Ki-67 immunoreactivity from previous cell-cycle events, we further verified our results by using single-cell RT-PCR to detect *Ki-67* mRNA in GFP-positive cells. GFP-positive cells in the SVZ of the E18 neocortex were dissected (Fig. 2A,B), dissociated into single cells, identified by their GFP fluorescence and picked up one by one by aspiration through a glass capillary pipette (Esumi et al., 2008). The total RNA obtained from a single cell was converted into cDNA and amplified by nested PCR. To detect only cDNA, the PCR primers were designed to span more than one intron (see Table S1 in the supplementary material). Almost all of the 54 β-actin-positive cells expressed *Gad1* mRNA, and a significant fraction (10/54) also expressed *Mki67* mRNA (Fig. 3A; see Table S2 in the supplementary material).

Single-cell RT-PCR is useful for detecting the mRNAs co-expressed in a single cell. However, the number of genes detectable by this method in a single cell is, at best, limited to 10. Therefore, we also profiled the gene expression by single GFP-positive cells using single-cell microarray analysis (Esumi et al., 2008). Although the array data included almost the same number of false-Absent calls as Present calls, we did not encounter any false-Present calls. Moreover, we increased the reliability of the array data by examining the expression of important genes by immunohistochemistry or single-cell RT-PCR using amplified cDNA samples as the template.

Of the neuronal markers, we noted that *Tα1 tubulin* (*Tuba1* – Mouse Genome Informatics) had Present calls in 10 out of 10 cells, and doublecortin (*Dcx*) in nine cells (Fig. 3B). *Gad1* cDNA was also detected in all 10 cells by single-cell RT-PCR and by single-cell quantitative RT-PCR (Esumi et al., 2008), confirming that these cells were neurons or neuronal precursors. Some had differentiated into a GABAergic neuronal subtype, as indicated by Present calls for *Npy* and *Reln* (Fig. 3B). We also noted that many genes related to DNA replication had Present calls in a number of cells (Fig. 3C; see Table S3 in the supplementary material). In particular, cell #2 had Present calls for *Pcna*, cyclin D2 (*Ccnd2* – Mouse Genome Informatics) (Glickstein et al., 2009), cyclin E1 (Ccne1) and cyclin E2 (Ccne2), and cell #4 had Present calls for cyclin D1 (*Ccnd1*) and cyclin D2 (Fig. 3D). Cell #2 also had a Marginal call for *Mki67*, which was expressed predominantly in the G1-S phase. To confirm the appearance of cyclin D1 in the GAD67-GFP-positive cells, we performed immunohistochemistry (see Fig. S5 in the supplementary material). From the gene-expression profiling, we speculated that cells #2 and #4 were in S phase and G1 phase, respectively.

The single-cell gene-expression analyses also confirmed that the GAD67 and cell-cycle markers are co-expressed in the GFP-positive neuron precursors. In addition, we detected *Dcx* expression in cell #4 (Fig. 3B). Since *Dcx* is an essential gene expressed by precursors of excitatory neurons in the SVZ (Bai et al., 2003), nIPs migrating from the VZ to the SVZ may express Dcx, and maybe also IPGNs. Single-cell RT-PCR also showed that GFP-positive cells expressing *Mki67* and *Gad1* mRNAs often expressed the proneural gene *Mash1/Ascl1* (see Fig. S6 in the supplementary material). All the listed cells in the array analysis had Absent calls for the major glial markers (*Gfap*, *Cnp*, *Pdgfra*, *Plp1*).

To confirm further that the cell-cycle phases represented cell division and not apoptosis, we examined the expression of *E2f1*, a suppressor of cell-cycle entry (Wang et al., 2007). *E2f1* had a Present call in cell #10, which showed fewer Present calls for DNA-replication genes (Fig. 3D). In addition, we found no GFP-positive cells that co-expressed *E2f1* and *Mki67*, whereas one GFP-positive cell co-expressed delta-like 1 (*Dll1*) and *E2f1* (see Fig. S7 in the supplementary material), which may have been in the process of terminating cell division and differentiating into a neuron. In addition to *Dll1*, the array data indicated that genes related to asymmetric cell division, such as *Notch3*, delta-like 4 (*Dll4*) and *Numb* were also expressed by the GFP-positive cells. Immunohistochemistry also revealed Notch3 immunoreactivity and Dll4 immunoreactivity in one of a pair of GAD67-GFP-positive cells in close contact (Kageyama et al., 2009; Sprinzak et al., 2010) (see Figs S8, S9 in the supplementary material). The expression of these molecules is consistent with the idea that an IPGN divides in the neocortex to give rise a GABAergic neuron and to renew itself (see also Discussion).

Cell division of the IPGNs in vitro

To confirm that some of the GFP-positive cells in the GAD67-GFP mouse were IPGNs, we collected the GFP-positive cells with a fluorescence activated cell sorter (FACS) in culture medium (Fig. 4A-D). We tested several different culture conditions for growing the sorted cells and found that a medium for neural stem cells (Tropepe at al., 1999) did not induce proliferation (Fig. 4E). The

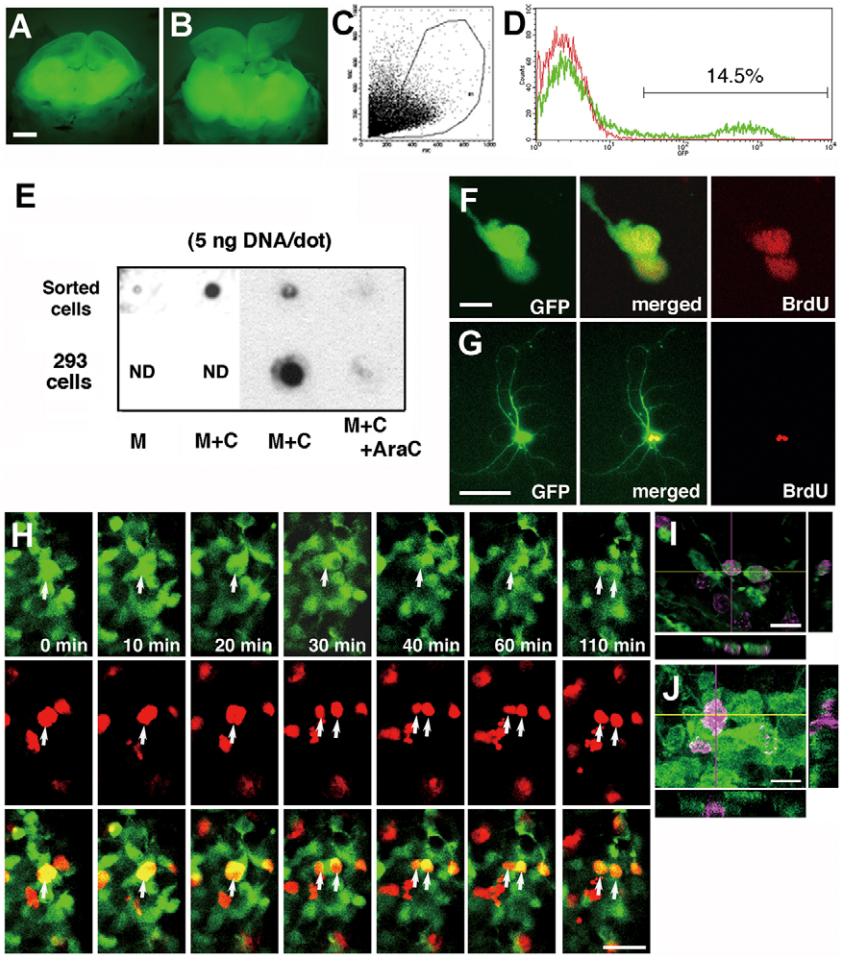

Fig. 4. Proliferation of GAD67/GFP-positive cells in vitro. (**A**,**B**) Dissection of the pallium from E18 GAD67-GFP knock-in mouse embryos. (**C**) Example of a fluorescence-activated cell sorting (FACS) profile for the GFP-positive cells. (**D**) Histogram showing the number of cells (*y*-axis) along with their fluorescence intensity (red, total cells; green, GFP-positive cells). (**E**) Dot-blot analysis showing BrdU incorporation in the DNA of the cells. M indicates GFP-positive cells cultured in medium for neural stem cells with BrdU. M+C indicates GFP-positive cells cultured in the medium conditioned with embryo brain tissue overnight and with BrdU. M+C+AraC indicates GFP-positive cells culture in the conditioned medium with BrdU and AraC. Control 293 cells were also cultured in the same medium and BrdU incorporation was detected. Both GFP-positive cells and 293 cells failed to incorporate BrdU in the presence of AraC. (**F**,**G**) Immunocytochemistry for GFP and BrdU in cultured GFP-positive cells. Sorted cells were cultured for 2-5 days in the conditioned medium with BrdU. After the time in culture, pairs of cells double-labeled for GFP and BrdU were often seen. In the 5-day culture, two GFP-positive, BrdU-positive cells in a pair extended axons and dendrites. (**H**) Division of a GFP-positive cell and a GFP/histone-H2B-mCherry fusion protein double-labeled cell, recorded by video-microscopy. (**I**,**J**) Immunohistochemical detection of BrdU (I) or P-H3 (J) in a cultured brain slice used for video-microscopy. Many double-positive cells were found in every experiment. Scale bars: 1 mm in A; 10 μm in F,I,J; 50 μm in G,H.

IPGNs proliferated in a medium conditioned with embryo telencephalic tissue, which provided unknown growth factors. The ability of the cells to incorporate BrdU in culture medium was sensitive to AraC (Fig. 4E), and, after 2 days in culture, a small number of GFP-positive cells were positive for BrdU (Fig. 4F). Most of the BrdU-positive cells were found in pairs. After 5 days in culture, the number of BrdU-positive cells had not increased, but they extended Tuj1-positive dendrites and axons (Fig. 4G).

We also recorded the division of GAD67-GFP-positive cells in brain slices by video microscopy (Fig. 4H; see Movies 1, 2 in the supplementary material). The cells were observed for up to 8 hours, during which scattered GFP-positive cells divided. The two daughter cells remained GFP-positive during our observation period. We also monitored their nuclear division by observing the red fluorescence of a histone-H2B-mCherry fusion protein (Kanda et al., 1998). After every video recording, we performed immunohistochemistry and confirmed the presence of P-H3 immunoreactivity and BrdU in the GFP-positive cells, demonstrating that BrdU had been incorporated from the culture medium into the nucleus, that the GFP-positive cells had divided, and therefore that the IPGNs in the brain slices proliferated in vitro (Fig. 4I,J).

Cell types generated from IPGNs as revealed by simple retrovirus transduction

Next, to prove the proliferation of the IPGNs and to trace the fate of the progeny of IPGNs in vivo, we produced GAD67-Cre knock-in mice (see Fig. S1 in the supplementary material) and crossed them with TVA Cre-reporter mice [which express TVA, an avian sarcoma leukosis virus (ASLV) receptor] (see Fig. S2 in the supplementary material). We used the resulting GAD67-Cre/tv-A progeny in the following experiments, in which GAD67-expressing cells were transduced by infection of replication-incompetent GFP-expressing simple retrovirus, a recombinant ASLV (Hughes et al., 1987).

A small amount of ASLV solution was injected into the parenchyma of the neocortex of 20 E15-P0 GAD67-Cre/tv-A mice. Proliferating GAD67-positive cells (i.e. IPGNs) were susceptible to retroviral infection, and they (Fig. 5A) and/or their descendents could be identified by GFP immunohistochemistry in the injected brains, which were recovered 4-7 days later. Their descendents included non-pyramidal neurons (five cells) in the neocortex (Fig. 5B), many migrating cells in the rostral migratory stream (RMS) (124 cells) (Fig. 5C), and granule (141 cells) and periglomerular (24 cells) cells in the olfactory bulb (Fig. 5D,E). From the distribution of labeled IPGNs and migrating cells in the RMS, we could roughly speculate the injection site in the neocortex (Fig. 5A, inset).

When virus was injected into the lateral ventricle, no labeled cells were seen; nor were any cells labeled in the brain of wild-type mice. However, the level of GFP expression from the recombinant ASLV DNA was not high enough for us to perform a subtype analysis of the nonpyramidal neurons in the neocortex or of the labeled cells in the olfactory bulb. We tried repeating this experiment in five Nkx2.1-Cre mice (Kessaris et al., 2006) mated

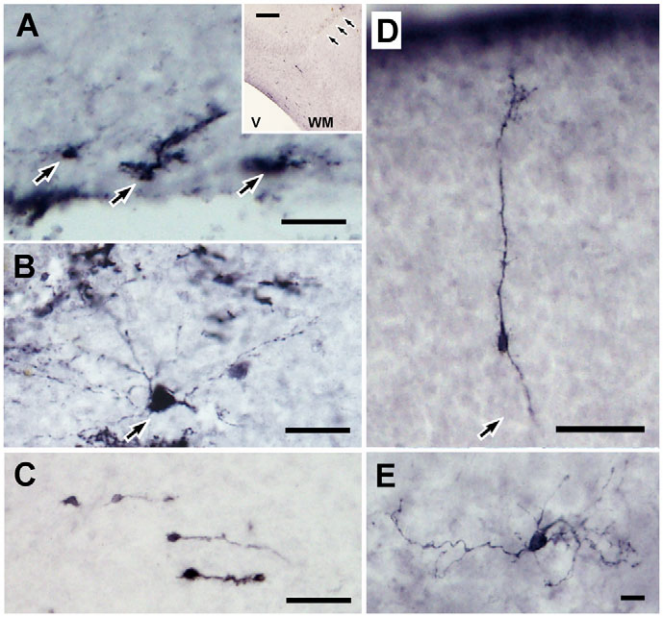

Fig. 5. Cells produced by IPGNs. The descendents of IPGNs were examined by labeling the IPGNs with a GFP-expressing simple retrovirus (the RCAS system). (**A-E**) Recombinant ASLV was injected into the parenchyma of the neocortex of GAD67-Cre/tvA or Nkx2.1-Cre/tvA mouse embryos at E15-P0 (inset in A). Four to 7 days later, the GFP-positive cells were revealed by immunohistochemistry. (A-C) IPGNs in the SVZ (A) and in a nonpyramidal neuron in the neocortex (B), and migrating cells in the RMS in GAD67-Cre/tvA mice (C). (D,E) A granule cell (D) and a periglomerular cell (E) in the olfactory bulb of a Nkx2.1-Cre/tvA mouse. V, lateral ventricle; WM, white matter. Arrows indicate capillary tract in the inset of A and somata in A,B,D. Scale bars: 100 μm (inset in A); 50 μm in A-D; 10 μm in E.

with TVA Cre-reporter mouse and found two nonpyramidal neurons in the neocortex, many migrating cells in the RMS (224 cells), as well as granule cells (120 cells) and periglomerular cells (35 cells) in the olfactory bulb.

Origin of the IPGNs as revealed by genetic neuroanatomy

Next, we examined the origin of the IPGNs in the embryonic neocortex using three different approaches. First, we introduced a GFP Cre-reporter plasmid with a floxed modified red fluorescent protein (mRFP)-stop into various parts of the telencephalic VZ of E14 GAD67-Cre mouse embryos by electroporation (Fig. 6A, plasmid 1). Depending on the placement of the electrodes, the transduced domain, which was identified by the mRFP fluorescence in the VZ, could be shifted along the ventral-to-dorsal axis (black arrows in Fig. 6B-D,G). When the electroporation site included the VZ of the ganglionic eminence (GE), the medial GE (MGE) could be distinguished from the rest of the structure, by its green fluorescence (Fig. 6B,C), whereas the lateral GE (LGE) emitted intense red fluorescence throughout the observation period. In fact, the transduced cells in the LGE were positive for both GFP and mRFP. However, the cells in the SVZ of the MGE may have a higher GAD67 promoter activity than those in the LGE (Tamamaki et al., 2003a), so the Cre recombinase in the MGE may have deleted more floxed mRFP cDNA than in the LGE. Thus, we assumed that the green cells (white arrows in Fig. 6C,D) originated in the MGE and the red cells in the LGE (Fig. 6D, inset). Four days after the electroporation, many green and red cells were observed in the dorsal neocortex and the hippocampus (Fig. 6D).

Next, we autoclaved the sections to eliminate the mRFP fluorescence and detected GFP and Ki-67 by immunohistochemistry. GFP-positive cells in the neocortical SVZ were often positive for Ki-67 immunoreactivity (7/69) (Fig. 6E,F). As these GFP-positive cells were in the GAD67-positive cell lineage, we regard these GFP/Ki-67 double-positive cells in the SVZ as IPGNs. This experiment indicates that IPGNs in the neocortical SVZ at P0 originate in the MGE and LGE. When we introduced the GFP Cre-reporter plasmid into the VZ of the dorsal neocortex at E14 and examined the brain at E18, no green cells were seen in the neocortex (Fig. 6G,H).

Next, we repeated the experiment described above, but used a plasmid in which fluorescent ubiquitylation-based cell cycle indicator-green (Fucci-G) cDNA (Sakaue-Sawano et al., 2008) was used instead of GFP (Fig. 6A, plasmid 2), and another in which the GFP cDNA was replaced with CFP cDNA (Fig. 6A, plasmid 3). Cre-positive cells in the GE delete the floxed mRFP-stop cassette and transcribe the Fucci-G and CFP cDNAs into mRNAs. As Fucci-G cDNA encodes a modified AzamiGreen (mAG) fused with a Geminin fragment, a cell in S-G2-M phase accumulates Fucci-G protein in the nuclei (Fig. 6J,K), but one in the G1 and G0 phases removes Fucci-G by degradation and appears as an mRFP- and CFP-double-positive cell (Fig. 6K). After the transduction of the VZ cells in the GE with the Fucci-G and CFP-Cre-reporter plasmids, cells triple-labeled for Fucci-G, mRFP and CFP were found in the GE, neocortex and hippocampus (see Fig. S10 in the supplementary material). mRFP-labeled cells lined up the cell migration stream in the LGE (arrows in K) (Fig. 6K). About 10-20% of the mRFP-positive cells were positive for Fucci-G at E18 (Fig. 6J). These Fucci-G-positive cells were also positive for Dcx immunoreactivity (Fig. 6L). As the Fucci-G-positive cells belonged to the GAD67-positive cell lineage and were in the S-G2-M phases, we regarded them as IPGNs.

When the plasmids for the CFP Cre-reporter and Fucci-G expression (Fig. 6A, plasmid 3 and 4) were introduced into the LGE and MGE in Nkx2.1-Cre mouse embryos at E14, we found cells that were triple-labeled for mRFP, Fucci-G and CFP, and cells that were double-labeled for mRFP and Fucci-G in the neocortical SVZ at E16-E18 (Fig. 6M,N). We speculated that the former cells expressed Cre and originated in the MGE. The latter did not express Cre but express Fucci-G in the LGE. As both of cells were positive for Fucci-G and Dcx immunoreactivity, we regarded them as IPGNs.

Third, we mapped the contributions of different VZ regions to the production of IPGNs in the neocortex by using a battery of transgenic mice that express Cre in defined neuroepithelial domains: Nkx2.1-Cre (MGE) (Kessaris et al., 2006) and Gsh2-Cre (MGE and LGE) (Kessaris et al., 2006), and Emx1-Cre (cerebral cortex) (Iwasato et al., 2000). These mice were crossed to a GFP Cre-reporter (Novak et al., 2000) to label the progeny originating from each Cre-expressing domain. Next, we immunostained sections for GABA immunoreactivity and Ki-67 immunoreactivity on the GFP-positive cells in the neocortex of all three genotypes of mice at P0. In the Nkx2.1-Cre/GFP and Gsh2-Cre/GFP mice, GABA immunoreactivity was frequently seen on GFP-positive cells in the neocortical SVZ and IZ. In the NKx2.1-Cre/GFP mice, the percentages of double-labeled cells among GFP-positive and GABA-positive cells in the SVZ and IZ were 24.4% and 16.4%, respectively (Fig. 7A,H). In the

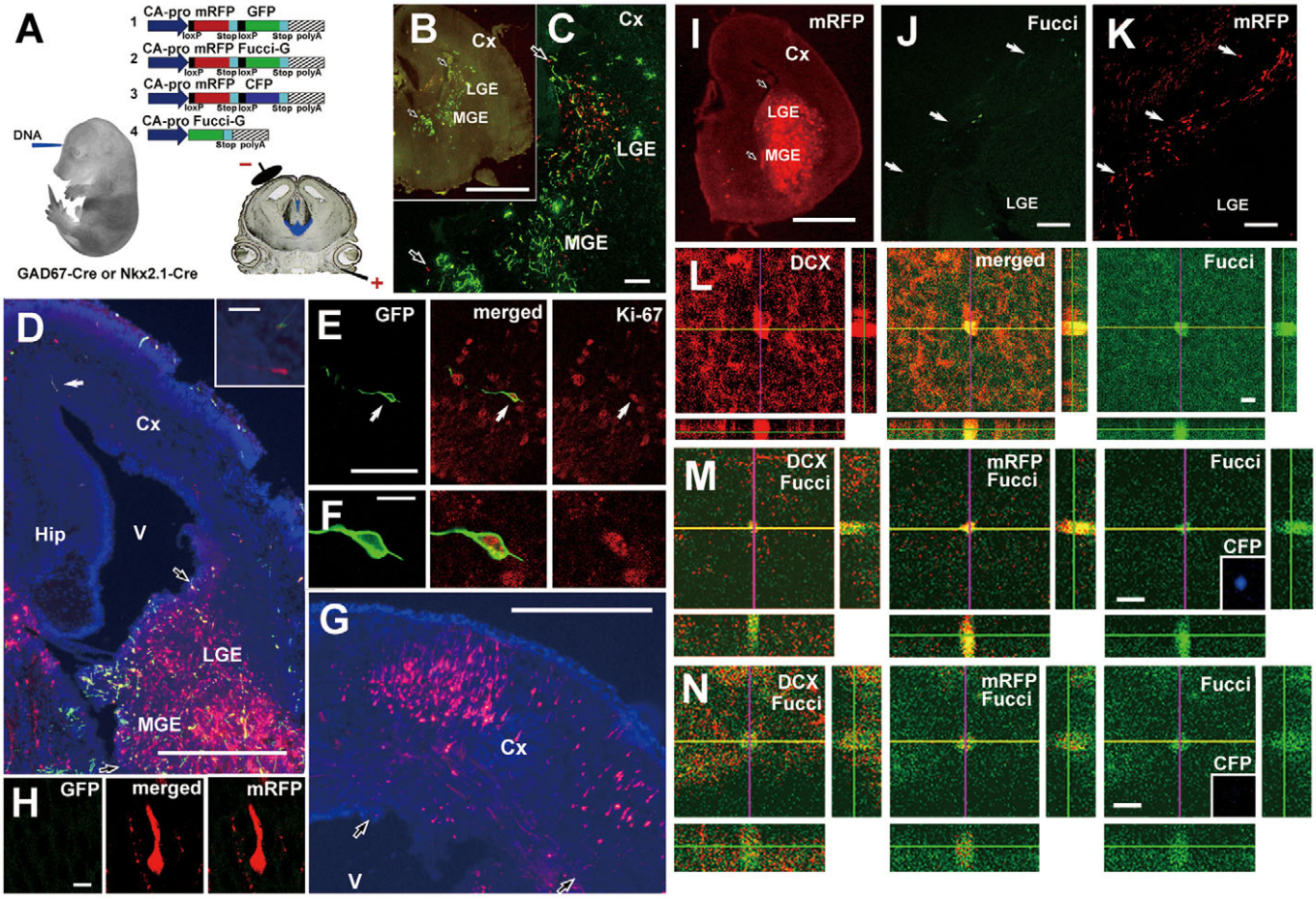

Fig. 6. Origin of the IPGNs assessed by transduction of the telecephalic VZ with Cre-reporter plasmids. (**A**) Constructs used to transduce VZ cells of GAD67-Cre and Nkx2.1-Cre mouse embryos. (1-3) GFP, Fucci and CFP Cre-reporter plasmids with floxed mRFP-stop. (4) A Fucci-G expression plasmid. (**B**,**C**) Ganglionic eminence (GE) of E16 mouse embryo expressing GFP by transduction with GFP Cre-reporter plasmid (1). Green and red cells are visible. (**D**) Neocortex at E18 shows green and red cells that had migrated tangentially from the GE (D and inset). Most green (GFP-positive) cells expressed a small amount of mRFP, and vice versa. (**E**,**F**) Some GFP-positive cells in the neocortical SVZ (7/69) expressed Ki-67. (**G**,**H**) When the neocortical VZ was transduced with the same plasmid at the locations indicated by the arrows in G, no GFP-positive cells were found in the telencephalon (H). (**I-L**) When Fucci-G and CFP Cre-reporters (2 and 3) were introduced into the GE (I), mRFP-positive migrating cells (K) were found along the ventricular surface (white arrows). About 10-20% (8/43 in the figure) of the mRFP-positive cells was also positive for Fucci-G (J). The Fucci-G and mRFP-double-positive cells in the neocortex were also positive for Dcx (L). (**M**,**N**) Plasmids of CFP Cre-reporter and Fucci-G expression (3 and 4) were introduced to the ganglionic eminence of Nkx2.1-Cre mouse at E14. Embryos were recovered at E16 and observed. mRFP/Fucci-G/CFP triple-labeled cells (M) and mRFP/Fucci-G double-labeled cells (N) were found in the neocortical SVZ. These cells were positive for Dcx. Scale bars: 1 mm in B,I; 500 μm in D,G; 200 μm in J,K; 100 μm in C; 50 μm in the insets in D; 50 μm in E; 10 μm in F,H,L,M,N.

Gsh2-Cre/GFP mice, these percentages were 19.3% and 54.4%, respectively (Fig. 7B,G). In the dorsal neocortical SVZ of Emx1-Cre/GFP mice, we could not clearly detect any double-labeled cells in above-background fluorescence, although some may have migrated into the dorsal neocortex from the pallial-subpallial boundary (B) (Kohwi et al., 2007). As about 20% of the GABA-positive cells in the neocortical SVZ at P0 are IPGNs (see above), we examined whether Ki-67 immunoreactivity and GABA immunoreactivity were colocalized in GFP-positive cells in the Nkx2.1-Cre/GFP and Gsh2-Cre/GFP mouse neocortex. Our results revealed many triple-labeled cells (Fig. 7C-F). The results indicate that IPGNs originate in LGE or MGE, or both. Based on the data obtained from these three different experiments, we conclude that IPGNs in the neocortical SVZ originate in the MGE and LGE.

Fate of IPGNs after birth

To follow the fate of the IPGNs in the neocortical SVZ, we monitored them for up to 6 weeks after birth in the GAD67-GFP knock-in, GAD67-Cre/GFP, Nkx2.1-Cre/GFP, Gsh2-Cre/GFP and Emx1-Cre/GFP mice. As the GAD67-GFP mice grew, the GFP-positive cells in the neocortical SVZ gathered and formed cell clusters, which appeared as cell chains in successive sections and were negative for NeuN immunoreactivity (Fig. 8A). The GFP-positive cells in the cell chains were also positive for Dcx (see Fig. S11 in the supplementary material), GABA and GAD67 immunoreactivity (Tamamaki et al., 2003a). In addition, they were surrounded by GFAP-positive processes, as shown previously in the SVZ of the lateral wall of the lateral ventricle (Alvarez-Buylla and Garcia-Verdugo, 2002) (Fig. 8B). These observations were reminiscent of migrating young neurons (A cells) in the RMS.

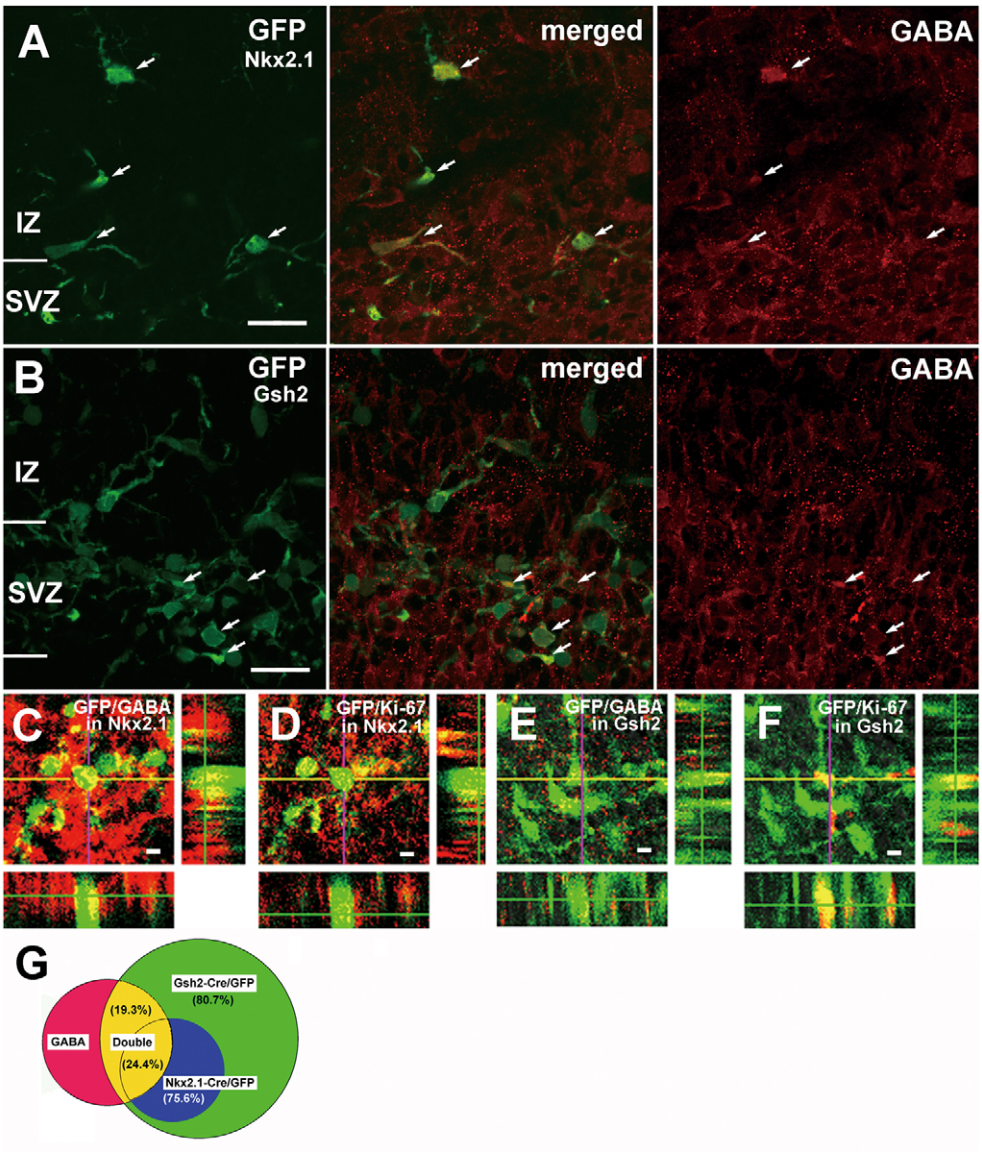

Fig. 7. IPGNs with subpallial markers are found in the neocortex. (**A**,**B**) We found many GABA and GFP double-labeled cells (indicated by arrows) in the neocortical SVZ and IZ of the Nkx2.1-Cre/GFP (A) and Gsh2-Cre/GFP (B) mice at P0. (**C-F**) Large numbers of the GABA/GFP double labeled cells were also positive for Ki-67 immunoreactivity in the Nkx2.1-Cre/GFP mice (C,D) and Gsh2-Cre/GFP mice (E,F). (**G**) Schematic diagram showing the proportion of GABA-positive cells in the P0 mouse that originated in the subpallium. Scale bars: 50 μm in A,B; 5 μm in C-F.

However, some of the GFP-positive cells in the chains were positive for Ki-67 immunoreactivity (Fig. 8C), which corresponds to the IPGNs characterized here. Therefore, Ki-67 immunoreactivity is co-localized with Dcx immunoreactivity, even in the wild-type mouse brain (see Fig. S11 in the supplementary material). These Ki-67-positive SVZ cells in the adult neocortex were reminiscent of transit-amplifying cells (C cells) (Doetsch et al., 2002). In fact, a C-cell marker, Mash1/Ascl1 immunoreactivity (Adachi et al., 2007), was often in close contact with GFP immunoreactivity in the GAD67-GFP mouse (see Fig. S12 in the supplementary material) (see Discussion). Moreover, their mRNA colocalized in the IPGNs (see Fig. S6 in the supplementary material).

To reveal the origin of the cells in the RMS in the dorsal neocortex, we examined GFP-positive cells in the adult neocortex of the Nkx2.1-Cre/GFP, Gsh2-Cre/GFP, Emx1-Cre/GFP and GAD67-Cre/GFP mice. We labeled brain sections for Dcx immunoreactivity and counted the number of Dcx/GFP-double-labeled cells (A cell + IPGNs) in the cell chains above the hippocampus (Fig. 8D-F). We found no Dcx immunoreactivity on the GFP-positive cells in the neocortical SVZ of the Nkx2.1-Cre/GFP mouse, (0/343) (Fig. 8D), possibly because the IPGNs in the neocortical SVZ, which originated in the MGE and produced granule cells for the olfactory bulb at perinatal stage (Fig. 5), may be exhausted at 6 weeks of age. In the Gsh2-Cre/GFP mice, the GFP-positive cells in the neocortical SVZ were small bipolar and often aligned in cell chains. The GFP-positive cells made up 45% (146/324) of the Dcx-positive cell in the dorsal-neocortex (Fig. 8E). In the Emx1-Cre/GFP mice, GFP-positive cells in the SVZ made up 19% (40/210) of the Dcx-positive cells in the dorsal neocortex (Fig. 8F). Although we could not determine the origin of 34% of the Dcx-positive cells in the dorsal neocortex, it is clear that a significant number of neurogenic IPGNs arrive in the dorsal neocortex from the MGE, LGE and maybe also from pallial-subpallial boundary (Emx1 cell-lineage), as well as additional unknown areas of the telencephalon, to produce the young neurons populating the RMS (Kriegstein and Alvarez-Buylla, 2009; Kohwi et al., 2007; Seri et al., 2006; Young et al., 2007; Lledo et al., 2008).

Besides migrating in the telencephalon and producing neocortical GABAergic neurons and olfactory granule cells, IPGN-like GFP-positive cells were often found along the neocortical SVZ

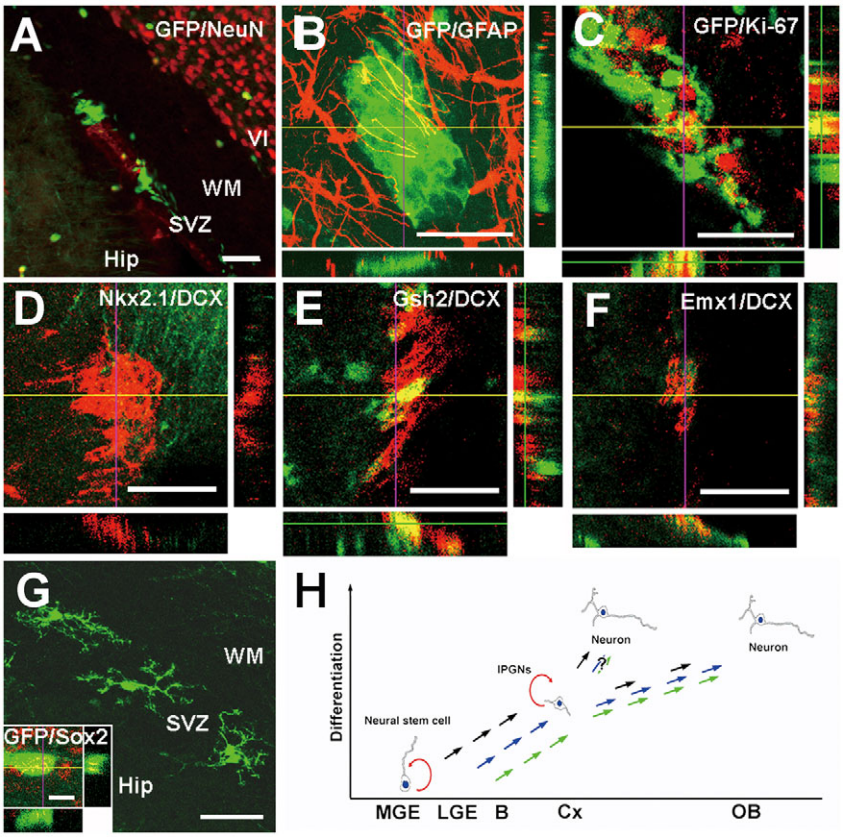

Fig. 8. Fate of IPGNs after birth. (**A**) GFP-positive cells in the SVZ of the GAD67-GFP mouse were still visible in the adult, and most were negative for NeuN. (**B**) GAD67-GFP-positive cells in the neocortical SVZ formed clusters and were surrounded by GFAP-positive processes. (**C**) Some of the GFP-positive cells were positive for Ki-67 immunoreactivity and in close contact with Mash1/Ascl1-positive cells (see Fig. S12 in the supplementary material). (**D**) A GFP-positive cell cluster is a part of the cell chains in the RMS. The cell chains are identified by Dcx immunoreactivity. The cell chains in the dorsal neocortex did not contain any GFP-positive cells in the Nkx2.1-Cre/GFP mouse. (**E**) GFP-positive cells in the Gsh2-Cre/GFP mice make up 45% (146/324) of the Dcx-positive cells in the neocortical cell chains. (**F**) GFP-positive cells in Emx1-Cre/GFP mice make up 19% (40/210) of the Dcx-positive cells in the neocortical cell-chains. (**G**) Some GFP-positive cells in the SVZ of GAD67-Cre/GFP mice appear to be IPGNs (Fig. 5A). They often showed Sox2 immunoreactivity (inset of G). (**H**) A schematic drawing summarizing the origin, differentiation and migration of the IPGNs, and the production of neurons by IPGNs. Scale bars: 100 μm in A; 50 μm in B-G; 10 μm in the inset in G.

of GAD67-Cre mice (Fig. 8G; compare with Fig. 5A). These IPGN-like cells often showed SOX2 immunoreactivity (inset in Fig. 8G). These Sox2-positive cells (Pevny and Nicolis, 2010) may be IPGNs that have settled in the neocortex and are reserved for neurogenesis in the case of brain damage or other pathology (Ohira et al., 2010). A schematic diagram summarizes our findings on the origin, differentiation and migration of IPGNs, and their progenies (Fig. 8H).

DISCUSSION

Origin and migration of IPGNs

It is well known that neocortical GABAergic neurons originate in the subpallium of rodents telencephalon (Anderson et al., 1997; Tamamaki et al., 1997), specifically in the MGE (Lavdas et al., 1999), LGE (Fogarty et al., 2007) and caudal GE (Nery et al., 2002), and are supplied by tangential migration to the pallium during embryonic stages. The supply of GABAergic neurons to the neocortex ends as the mouse grows and the distance between these structures increases. Under normal conditions, most of the brain regions may not require new neurons during the adult life of an animal. However, the ratio of GABAergic neurons in the adult neocortex is fixed at about 15-25%, depending on the brain area (Jones 1993; Tamamaki et al., 2003a), and a pathological change in the brain could cause disproportionate damage to the GABAergic versus excitatory neurons. If there were no way to add GABAergic neurons to the neocortex, brain function could be easily compromised. Therefore, although IPGNs may not be needed to populate the neocortex with GABAergic neurons during development, they may be required to adjust the ratio of GABAergic neurons by Notch-Delta-regulated proliferation in embryo brain and in adult brain under pathological conditions.

A few studies have reported the production of GABAergic neurons in the adult cerebral cortex (Liu et al., 2003; Ohira et al., 2010), but the origins of the progenitors for these neurons has been completely uncertain. The IPGNs described here are a likely source of GABAergic neuronal production in the adult cerebral cortex, even though they supply only a small number of GABAergic neurons to the neocortex of the perinatal brain, and primarily generate a large number of granule cells and periglomerular cells for the neonatal olfactory bulb. IPGNs in the adult brain have not been described, although labeling and tracing studies that should have marked them have been performed (Inta et al., 2008; Suzuki and Goldman, 2003). It is possible that their numbers are so low that IPGNs have not been recognized as a separate subpopulation or they may have been mis-identified as astrocytes, given their appearance (Fig. 5A).

Here, we have revealed that IPGNs in the neocortex originate in the subpallium (Figs 6 and 7), and we did not detect any GAD67-promoter-driven Cre expression in the VZ of the dorsal neocortex in E14-P0 mice (Fig. 6G,H). Our results support the idea that the VZ of the cerebral cortex cannot produce GABAergic neurons (Gorski et al., 2002). However, IPGNs also seemed to be produced at the pallial-subpallial boundary. Dcx-positive cells in the RMS of the dorsal neocortex comprised up to 19% of the GFP-positive cells in Emx1-Cre/GFP mouse and comprised completely GFP-positive cells in GAD67-GFP mouse (Fig. 8F; see Fig. S11 in the supplementary material). As the pallial-subpallial boundary is characterized by the expression of Dlx5/6 and Emx1 (Kohwi et al., 2007), IPGNs from the boundary may be in the Emx1 lineage but produce GABAergic young neurons for the olfactory bulb. Therefore, the IPGNs from the boundary may give rise the RMS cells in Emx1 lineage.

As IPGNs are not anchored by any radial fibers, IPGNs may be able to migrate randomly (Tabata et al., 2009) or one way when cued to do so and make a long journey even to the entire part of the cerebral cortex. The journey of the IPGNs from the pallium to the neocortex may be guided by the molecular mechanisms used by GABAergic young neurons (Marin et al., 2001; Tamamaki et al., 2003b).

Several cell migratory streams run in the embryonic brain and populate the various brain regions with many different types of neurons. Here, we examined a cell migratory stream extending from the GE to the neocortex and found IPGNs migrating in this stream. We speculate that the presence of neurogenic intermediate progenitors in this migratory stream is not unique, but just the first such example to be described.

Colocalization of GAD67 and Dcx with cell-cycle markers

In this study, we revealed characteristics of IPGNs that are different from those of neural stem cells. The generation of neurons from neural stem cells involves many differentiation steps. Previously, all of the differentiation steps were thought to occur in daughter cells arising from neural stem cells in the embryonic brain. However, nIPs (Kriegstein and Alvarez-Buylla, 2009) distribute the sequential differentiation steps among the cells in their lineage (Noctor et al., 2004; Miyata et al., 2004; Haubensak et al., 2004; Wu et al., 2005; Hansen et al., 2010; Letinic et al., 2002). The differentiation steps involve the expression of transcription factors for neuronal differentiation, of cytoskeletal and cell-adhesion molecules specific to neurons, and of molecules essential for neuron-specific function. During this process, some molecules are expressed in a phasic manner or gradually plateau. As none of the molecules show abrupt changes in expression, they are likely to overlap temporally and be colocalized in differentiating cells and asymmetrically dividing cells, even though their primary functions may be in distinct differentiation steps.

Recent studies show that the regulation of molecular expression during asymmetric cell division, such as Notch signaling, is more complex and dynamic than previously thought (Kageyama et al., 2009; Sprinzak et al., 2010), which helps explain why *Notch* and *Delta* are co-expressed in neuronal progenitors and daughter cells, and supports our observation that *Notch3*-positive cells in the neocortical SVZ at P0 also express Dll1 and Dll4 (Fig. 3E). Moreover, Mash1/Ascl1 immunoreactivity is used as a marker of C cells (Doetsch et al., 2002; Adachi et al., 2007). When a C cell divides and produces a C cell and an A cell for the olfactory bulb, and when markers of A cells are expressed in advance of the asymmetric cell division by leakage, the dividing C cells may contain the *Mash1/Ascl1*, *Ki-67* and *Gad1* mRNAs, as we detected by single-cell RT-PCR in the GFP-positive cells (see Fig. S6 in the supplementary material). Moreover, GABA may not be solely a transmitter stored in synaptic vesicles at the perinatal stages but might function as a regulator of cell proliferation (LoTurco et al., 1995; Haydar et al., 2000). In addition, when IPGNs preparing for asymmetric cell division are arrested in the S-G2-M phases for cell migration (Fig. 6J,K), cell-cycle markers and Dcx could accumulate in the same cell (Fig. 3B #4 cell).

The neural stem cells in the SVZ of the adult telencephalon (B cells) are the source of GABAergic granule cells and periglomerular cells in the olfactory bulb, and nIPs (C cells) assist to expand the neuron production. As the SVZ of the ventral wall of the lateral ventricle is completely occupied by B cells and C cells, some C cells may migrate from the subpallium to the dorsal neocortex to find an appropriate niche for neuron production. Thus, the IPGNs in the neocortex may be C cells that have accumulated GAD67 and Dcx during migration. Although we found IPGNs co-expressing *Gad1*, *Dcx* and cell-cycle markers, GAD67 and Dcx may not be unique; rather, different kinds of nIPs may accumulate different sets of molecules during migration (Luskin, 1998). In any case, we expect that further study of the IPGNs will show that neurogenesis in the embryonic stages and adult is, at least in part, a continuous event.

Acknowledgements

We thank Drs N. Kessaris, W. D. Richardson, T. Iwasato and C. G. Lobe for their donation of the Nkx2.1-Cre, Gsh2-Cre, Emx1-Cre and Z/G Cre-reporter mice. We also thank Drs T. Kanda, A. D. Leavitt, J. L. R. Rubenstein and R. Tsien for their donation of antibodies and cDNAs. This study was supported by a Grant-in-Aid for Scientific Research on Priority Area-Advanced Brain Science Project from the Ministry of Education, Culture, Sports, Science and Technology, Japan to N.T., and by a COE grant in IMEG in Kumamoto University and National Natural Science Foundation of China (No. 30970946) to S.W. The funding bodies had no role in the study design, data collection and analysis, decision to publish, or preparation of the manuscript.

Competing interests statement

The authors declare no competing financial interests.

Supplementary material

Supplementary material for this article is available at
http://dev.biologists.org/lookup/suppl/doi:10.1242/dev.063032/-/DC1

References

Adachi, K., Mirzadeh, Z., Sakaguchi, M., Yamashita, T., Nikolcheva, T., Gotoh, Y., Peltz, G., Gong, L., Kawase, T., Alvarez-Buylla, A. et al. (2007). Beta-catenin signaling promotes proliferation of progenitor cells in the adult mouse subventricular zone. *Stem Cells* **25**, 2827-2836.

Alvarez-Buylla, A. and Garcia-Verdugo, J. M. (2002). Neurogenesis in adult subventricular zone. *J. Neurosci.* **22**, 629-634.

Anderson, S. A., Eisenstat, D. D., Shi, L. and Rubenstein, J. L. R. (1997). Interneuron migration from the basal forebrain to the neocortex: dependence on Dlx genes. *Science* **278**, 474-476.

Bai, J., Ramos, R. L., Ackman, J. B., Thomas, A. M., Lee, R. V. and LoTurco, J. J. (2003). RNAi reveals doublecortin is required for radial migration in rat neocortex. *Nat. Neurosci.* **6**, 1277-1283.

Doetsch, F., Petreanu, L., Caille, I., Garcia-Verdugo, J. M. and Alvarez-Buylla, A. (2002). EGF converts transit-amplifying neurogenic precursors in the adult brain into multipotent stem cells. *Neuron* **36**, 1021-1034.

Englund, C., Fink, A., Lau, C., Pham, D., Daza, R. A., Bulfone, A., Kowalczyk, T. and Hevner, R. F. (2005). Pax6, Tbr2, and Tbr1 are expressed sequentially by radial glia, intermediate progenitor cells, and postmitotic neurons in developing neocortex. *J. Neurosci.* **25**, 247-251.

Esumi, S., Wu, S. X., Yanagawa, Y., Obata, K., Sugimoto, Y. and Tamamaki, N. (2008). Method for single-cell microarray analysis and application to gene-expression profiling of GABAergic neuron progenitors. *Neurosci. Res.* **60**, 439-451.

Fogarty, M., Grist, M., Gelman, D., Marín, O., Pachnis, V. and Kessaris, N. (2007). Spatial genetic patterning of the embryonic neuroepithelium generates GABAergic interneuron diversity in the adult cortex. *J. Neurosci.* **27**, 10935-10946.

Glickstein, S. B., Monaghan, J. A., Koeller, H. B., Jones, T. and Ross, M. E. (2009). Cyclin D2 is critical for intermediate progenitor cell proliferation in the embryonic cortex. *J. Neurosci.* **29**, 9614-9624.

Gorski, J. A., Talley, T., Qiu, M., Puelles, L., Rubenstein, J. L. and Jones, K. R. (2002). Cortical excitatory neurons and glia, but not GABAergic neurons, are produced in the Emx1-expressing lineage. *J. Neurosci.* **22**, 6309-6314.

Hansen, D. V., Lui, J. H., Parker, P. R. and Kriegstein, A. R. (2010). Neurogenic radial glia in the outer subventricular zone of human neocortex. *Nature* **464**, 554-561.

Haubensak, W., Attardo, A., Denk, W. and Huttner, W. B. (2004). Neurons arise in the basal neuroepithelium of the early mammalian telencephalon: a major site of neurogenesis. *Proc. Natl. Acad. Sci. USA* **101**, 3196-3201.

Haydar, T. F., Wang, F., Schwartz, M. L. and Rakic, P. (2000). Differential modulation of proliferation in the neocortical ventricular and subventricular zones. *J. Neurosci.* **20**, 5764-5774.

Herrup, K. and Yang, Y. (2007). Cell cycle regulation in the postmitotic neuron: oxymoron or new biology? *Nat. Rev. Neurosci.* **8**, 368-378.

Hughes, S. H., Greenhouse, J. J., Petropoulos, C. J. and Sutrave, P. (1987). Adaptor plasmids simplify the insertion of foreign DNA into helper-independent retroviral vectors. *J. Virol.* **61**, 3004-3012.
Inta, D., Alfonso, J., von Engelhardt, J., Kreuzberg, M. M., Meyer, A. H., van Hooft, J. A. and Monyer, H. (2008). Neurogenesis and widespread forebrain migration of distinct GABAergic neurons from the postnatal subventricular zone. *Proc. Natl. Acad. Sci. USA* **105**, 20994-20999.
Iwasato, T., Datwani, A., Wolf, A. M., Nishiyama, H., Taguchi, Y., Tonegawa, S., Knöpfel, T., Erzurumlu, R. S. and Itohara, S. (2000). Cortex-restricted disruption of NMDAR1 impairs neuronal patterns in the barrel cortex. *Nature* **406**, 726-731.
Jones, E. G. (1993). GABAergic neurons and their role in cortical plasticity in primates. *Cereb. Cortex* **3**, 361-372.
Kageyama, R., Ohtsuka, T., Shimojo, H. and Imayoshi, I. (2009). Dynamic regulation of Notch signaling in neural progenitor cells. *Curr. Opin. Cell Biol.* **21**, 733-740.
Kanda, T., Sullivan, K. F. and Wahl, G. M. (1998). Histone-GFP fusion protein enables sensitive analysis of chromosome dynamics in living mammalian cells. *Curr. Biol.* **26**, 377-385.
Kessaris, N., Fogarty, M., Iannarelli, P., Grist, M., Wegner, M. and Richardson, W. D. (2006). Competing waves of oligodendrocytes in the forebrain and postnatal elimination of an embryonic lineage. *Nat. Neurosci.* **9**, 173-179.
Kohwi, M., Petryniak, M. A., Long, J. E., Ekker, M., Obata, K., Yanagawa, Y., Rubenstein, J. L. and Alvarez-Buylla, A. (2007). A subpopulation of olfactory bulb GABAergic interneurons is derived from Emx1- and Dlx5/6-expressing progenitors. *J. Neurosci.* **27**, 6878-6891.
Kriegstein, A. and Alvarez-Buylla, A. (2009). The glial nature of embryonic and adult neural stem cells. *Annu. Rev. Neurosci.* **32**, 149-184.
Lavdas, A. A., Grigoriou, M., Pachnis, V. and Parnavelas, J. G. (1999). The medial ganglionic eminence gives rise to a population of early neurons in the developing cerebral cortex. *J. Neurosci.* **19**, 7881-7888.
Letinic, K., Zoncu, R. and Rakic, P. (2002). Origin of GABAergic neurons in the human neocortex. *Nature* **417**, 645-649.
Liu, S., Wang, J., Zhu, D., Fu, Y., Lukowiak, K. and Lu, Y. M. (2003). Generation of functional inhibitory neurons in the adult rat hippocampus. *J. Neurosci.* **23**, 732-736.
Lledo, P. M., Merkle, F. T. and Alvarez-Buylla, A. (2008). Origin and function of olfactory bulb interneuron diversity. *Trends Neurosci.* **31**, 392-400.
LoTurco, J. J., Owens, D. F., Heath, M. J., Davis, M. B. and Kriegstein, A. R. (1995). GABA and glutamate depolarize cortical progenitor cells and inhibit DNA synthesis. *Neuron* **15**, 1287-1298.
Luskin, M. B. (1998). Neuroblasts of the postnatal mammalian forebrain: their phenotype and fate. *J. Neurobiol.* **36**, 221-233.
Marín, O., Yaron, A., Bagri, A., Tessier-Lavigne, M. and Rubenstein, J. L. (2001). Sorting of striatal and cortical interneurons regulated by semaphorin-neuropilin interactions. *Science* **293**, 872-875.
Miyata, T., Kawaguchi, A., Okano, H. and Ogawa, M. (2001). Asymmetric inheritance of radial glial fibers by cortical neurons. *Neuron* **31**, 727-741.
Miyata, T., Kawaguchi, A., Saito, K., Kawano, M., Muto, T. and Ogawa, M. (2004). Asymmetric production of surface-dividing and non-surface-dividing cortical progenitor cells. *Development* **131**, 3133-3145.
Nery, S., Fishell, G. and Corbin, J. G. (2002). The caudal ganglionic eminence is a source of distinct cortical and subcortical cell populations. *Nat. Neurosci*. **5**, 1279-1287.
Noctor, S. C., Flint, A. C., Weissman, T. A., Dammerman, R. S. and Kriegstein, A. R. (2001). Neurons derived from radial glial cells establish radial units in neocortex. *Nature* **409**, 714-720.
Noctor, S. C., Martinez-Cerdeno, V., Ivic, L. and Kriegstein, A. R. (2004). Cortical neurons arise in symmetric and asymmetric division zones and migrate through specific phases. *Nat. Neurosci.* **7**, 136-144.
Novak, A., Guo, C., Yang, W., Nagy, A. and Lobe, C. G. (2000). Z/EG, a double reporter mouse line that expresses enhanced green fluorescent protein upon Cre-mediated excision. *Genesis* **28**, 147-155.
Ohira, K., Furuta, T., Hioki, H., Nakamura, K. C., Kuramoto, E., Tanaka, Y., Funatsu, N., Shimizu, K., Oishi, T., Hayashi, M. et al. (2010). Ischemia-induced neurogenesis of neocortical layer 1 progenitor cells. *Nat. Neurosci.* **13**, 173-179.
Pevny, L. H. and Nicolis, S. K. (2010). Sox2 roles in neural stem cells. *Int. J. Biochem. Cell Biol.* **42**, 421-424.
Sakaue-Sawano, A., Kurokawa, H., Morimura, T., Hanyu, A., Hama, H., Osawa, H., Kashiwagi, S., Fukami, K., Miyata, T., Miyoshi, H. et al. (2008). Visualizing spatiotemporal dynamics of multicellular cell-cycle progression. *Cell* **132**, 487-498.
Seri, B., Herrera, D. G., Gritti, A., Ferron, S., Collado, L., Vescovi, A., Garcia-Verdugo, J. M. and Alvarez-Buylla, A. (2006). Composition and organization of the SCZ: a large germinal layer containing neural stem cells in the adult mammalian brain. *Cereb. Cortex* **16**, i103-i111.
Sprinzak, D., Lakhanpal, A., Lebon, L., Santat, L. A., Fontes, M. E., Anderson, G. A., Garcia-Ojalvo, J. and Elowitz, M. B. (2010). Cis-interactions between Notch and Delta generate mutually exclusive signalling states. *Nature* **465**, 86-90.
Suzuki, S. O. and Goldman, J. E. (2003). Multiple cell populations in the early postnatal subventricular zone take distinct migratory pathways: a dynamic study of glial and neuronal progenitor migration. *J. Neurosci.* **23**, 4240-4250.
Tabata, H., Kanatani, S. and Nakajima, K. (2009). Differences of migratory behavior between direct progeny of apical progenitors and basal progenitors in the developing cerebral cortex. *Cereb. Cortex* **19**, 2092-2105.
Tamamaki, N., Fujimori, K. and Takauji, R. (1997). Origin and route of tangentially migrating neurons in the developing neocortical intermediate zone. *J. Neurosci.* **17**, 8313-8323.
Tamamaki, N., Nakamura, K., Okamoto, K. and Kaneko, T. (2001). Radial glia is a progenitor of neocortical neurons in the developing cerebral cortex. *Neurosci. Res.* **41**, 51-60.
Tamamaki, N., Yanagawa, Y., Tomioka, R., Miyazaki, J., Obata, K. and Kaneko, T. (2003a). Green fluorescent protein expression and colocalization with calretinin, parvalbumin, and somatostatin in the GAD67-GFP knock-in mouse. *J. Comp. Neurol.* **467**, 60-79.
Tamamaki, N., Fujimori, K., Nojyo, Y., Kaneko, T. and Takauji, R. (2003b). Evidence that Sema3A and Sema3F regulate the migration of GABAergic neurons in the developing neocortex. *J. Comp. Neurol.* **455**, 238-248.
Tropepe, V., Sibilia, M., Ciruna, B. G., Rossant, J., Wagner, E. F. and van der Kooy, D. (1999). Distinct neural stem cells proliferate in response to EGF and FGF in the developing mouse telencephalon. *Dev. Biol.* **208**, 166-188.
Wang, L., Wang, R. and Herrup, K. (2007). E2F1 works as a cell cycle suppressor in mature neurons. *J. Neurosci.* **27**, 12555-12564.
Wu, S. X., Goebbels, S., Nakamura, K., Nakamura, K., Kometani, K., Minato, N., Kaneko, T., Nave, K. A. and Tamamaki, N. (2005). Pyramidal neurons of upper cortical layers generated by NEX-positive progenitor cells in the subventricular zone. *Proc. Natl. Acad. Sci. USA* **102**, 17172-17177.
Young, K. M, Fogarty, M., Kessaris, N. and Richardson, W. D. (2007). Subventricular zone stem cells are heterogeneous with respect to their embryonic origins and neurogenic fates in the adult olfactory bulb. *J. Neurosci.* **27**, 8286-8296.
Yun, K., Fischman, S., Johnson, J., Hrabe de Angelis, M., Weinmaster, G. and Rubenstein, J. L. (2002). Modulation of the notch signaling by Mash1 and Dlx1/2 regulates sequential specification and differentiation of progenitor cell types in the subcortical telencephalon. *Development* **129**, 5029-5040.

Table S1. A list of primers used in this study

Gene	Primer	Product size	GenBank Accession Number
g67-2	5′-TTCCGGAGGTACCACACCTT-3′		
g67-5	5′-TAAGTCGACGCTAGCGAGCGCCTCCCCA-3′		
CreR1	5′-TTGCCCCTGTTTCACTATCC-3′		
Dll1	5'-TGTGGACCTCGGCAACTCTT-3'	570 bp	NM_007865
	5'-GCCCCAATGATGCTAACAGA-3'		
	5'-TGGCTACACGGGCAAGAACT-3'	295 bp	
	5'-GCAGACCACCACAGCAGCAC-3'		
Dll4	5'-TTAAGCACTTCCAGGCAACC-3'	584 bp	NM_019454
	5'-GTGGGGGATACATTCATTGC-3'		
	5'-ACCAACTCCTTCGTCGTCAG-3'	355 bp	
	5'-CATCTGGCTGGCACTCATAA-3'		
E2f1	5'-GCAACTGCTTTCGGAGGACT-3'	516 bp	NM_007891
	5'-GGTGGGGAGAGGCTGATGAA-3'		
	5'-CCAGGACCTTCG CAGCATTG-3'	278 bp	
	5'-CTGGGGATGTGGAGGGAGGT-3'		
GAD67 (*Gad1*)	5'-GCACCCGTGTTTGTTCTCAT-3'	559 bp	Z49976
	5'-TGTGAGGGTTCCAGGTGACT-3'		
	5'-TCCCAGAAGTGAAGACAAAAA-3'	380 bp	
	5'-TCTATGCCGCTGAGTTTGTG-3'		
Ki-67 (*Mki67*)	5'-CAACATTACAAAGCAAAAGCA-3'	675 bp	X82786
	5'-GCTTAGGTTCACTGTCCAAA-3'		
	5'-CACCAAAGCAGGAAGCAACA-3'	380 bp	
	5'-TTGGCCCCGAGATGTAGATT-3'		
Map2	5'-CTCCATCTCTTCAGCACGAC-3'	537 bp	M21041
	5'-GGTACGTGGTGAGCATTGTC-3'		
	5'-ACCCCGAGCTACCCCAGGAC-3'	294 bp	
	5'-ACCTGGCCTGTGACGGATGT-3'		
Notch3	5'-AGCTCGGGGCACGGACTGAC-3'	537 bp	NM_008716
	5'-GGGGCAGCCTGTCCAAGTGAT-3'		
	5'-CTGGATGCTGGGGCGGACAC-3'	352 bp	
	5'-GCGGCGTCTCTTCCTTGCTG-3'		
βIII-Tubulin	5'-AGTGCGGCAACCAGATAGGG-3'	609 bp	NM_023279
	5'-TGCGGAAGCAGATGTCGTAG-3'		
	5'-TCTGGCGCCTTTGGACACCT-3'	323 bp	
	5'-GCGTTGTAGGGCTCCACCAC-3'		
β-Actin	5'-GCCAACCGTGAAAAGATGAC-3'	556 bp	X03672
	5'-GCACTGTGTTGGCATAGAGG-3'		
	5'-GGCTGTGCTGTCCCTGTATG-3'	391 bp	
	5'-CAAGAAGGAAGGCTGGAAAA-3'		

β-Actin mRNA was detected by PCR to check the recovery of a single cell. The upper and lower primers were designed in different exons not to amplify genome DNA. In every experiment, extracellular bathing solution was collected as a control solution and used as a template for PCR. All PCR products were cloned in a cloning vector, pCRII (Invitrogen, USA), and sequenced.

Table S2. Summary of neuronal and cell-cycle markers detected on GFP-positive cells at E18

	Immunohistochemistry	Immunocytochemistry	Single-cell RT-PCR
Neuronal marker			
GABA	100% (254/254)	100% (551/551)	
GAD67	100% (289/289)	100% (668/668)	100% (54/54)
Map2	96% (231/240)	98.3% (339/345)	100% (54/54)
Tuj1(βIIITublin)	100% (171/171)	98.9% (471/476)	98.2% (53/54)
Dcx	98.3% (634/645)	100% (298/298)	ND
NCAM	100% (693/693)	100% (207/207)	ND
Dlx2	100% (56/56)	ND	ND
Cell-cycle marker			
Ki-67	25.4% (171/672)	14.4% (150/1041)	18.5% (10/54)
BrdU	1.5% (11/758)	0.76% (12/1582)	
pH3	ND	4.7% (64/1356)	
Nestin	ND	32% (331/1031)	ND

ND, no data.

Table S3. A list of genes that appear in Fig. 3

Gene symbol	Common gene name	Probe set ID	Accession Number
Neuronal marker			
Dcx	Doublecortin, Dcx	1418141_at	NM_001110222
Ncam1	NCAM-1, CD56,	1426864_a_at	NM_001081445
Tuba1a	Ta1, Tuba1a	1418884_x_at	NM_011653
Npy	Neuropeptide Y, Npy	1419127_at	NM_023456
Reln	Reelin, Reln	1449465_at	NM_011261
DNA replication-related genes			
Orc5l	Orc5,MmORC5	1415830_at	NM_011959
Nae1	59kDa, Appbp1	1423781_at	NM_144931
Ugcgl2	Ugcgl2	1431602_a_at	NM_001081252
Nfia	Nfia, NF1-A	1421163_a_at	NM_010905
Nfix	Nfix	1436363_a_at	NM_001081981
Nfib	Nfib	1448288_at	NM_008687
Nasp	Nasp, Epcs32	1416042_s_at	NM_001081475
Chaf1b	CAF1, CAF1A	1423877_at	NM_028083
Lig1	DNA ligaseI, LigI	1416641_at	NM_010715
Nfib	Nfib	1438244_at	NM_008687
Rfc5	Rfc5, Recc5, 36kDa	1452917_at	NM_028128
Tk1	Tk-1, Tk1a,Tk1b	1416258_at	NM_009387
Rrm2	R2, Rrm2	1434437_x_at	NM_009104
Dna2	Dna2l,Dna2	1438817_at	NM_177372
Rfc3	Recc3, Rfc3	1423700_at	NM_027009
Dut	dUTPase, Dutp, Dut	1419270_a_at	NM_023595
Mcm10	Mcm10	1433408_a_at	NM_027290
Rev3l	Rev, Rev3, Sez4	1424632_a_at	NM_011264
Fhit	Fra14A2, Fhit	1425893_a_at	NM_010210
Orc3l	Orc3, Orc3l	1416115_at	NM_015824
Med1	Med1, PBP, Pparbp	1421907_at	NM_001080118
Dock9	Dock9, Zizimin1	1444028_s_at	NM_001081039
akirin 2	Akirin 2	1428237_at	NM_001007589
Rpa1	Rpa1, Rpa, RF-A,	1437309_a_at	NM_026653
Fen1	Fen1, AW538437	1436454_x_at	NM_007999
Myst2	Hbo1, Hboa, KAT7	1447631_at	NM_177619
Rrm1	Rrm1, RnrM1	1415878_at	NM_009103
Rbbp4	Rbbp4, mRbAp48	1434892_x_at	NM_009030
Rfc4	Rfc4, A1, RFC37	1438161_s_at	NM_145480
Ssbp1	MtSSB, mtDBP	1452616_s_at	NM_028358
Tnfaip1	Edp1, Edp-1, Tnfip1	1417865_at	NM_009395
Orc4l	Orc4P, mMmORC4	1423336_at	NM_011958
Rfc1	Recc1, Alp145,	1451920_a_at	NM_011258
BC023882	D4S43h, BC023882	1423919_at	NM_146159
Orc6l	Orc6, Orc6l	1417037_at	NM_019716
Lig3	DNA ligase III, Lig3	1423419_at	NM_010716
Eif5b	IF2, Eif5b	1434604_at	NM_198303
Ccdc88a	Giv, Hkrp1, Girdin	1437216_at	NM_176841
Dnajc2	Zrf1, Zrf2, MIDA	1417657_s_at	NM_009584
Ssrp1	Hmg1-rs1, Hmgi-rs3,	1426788_a_at	NM_182990
Supt16h	Spt16, Fact140	1419741_at	NM_033618
Polb	DNA poly β, Polb	1434230_at	NM_011130
Rbbp7	Rbbp7, mRbAp46	1456227_x_at	NM_009031
Orc2l	Orc2, Orc2l	1418225_at	NM_001025378
Lin9	TGS, Bara, TGS1	1428639_at	NM_001103182
Poll	DNA poly λ, Poll	1449352_at	NM_020032
Rbms1	YC1, MSSP-1	1434005_at	NM_020296
Cyclins and cell proliferation markers			
Ccng2	Cyclin G2	1416488_at	NM_007635
Ccnt1	Cyclin T1	1419313_at	NM_009833
Ccnd2	Cyclin D2, Vin1, Vin-1	1455956_x_at	NM_009829
Ccne2	Cyclin E2	1422535_at	NM_001037134
Ccni	Cyclin I	1448334_a_at	NM_017367
Ccnd1	Cyclin D1, Cyl-1, bcl-1	1417420_at	NM_007631
Ccnl1	Cyclin L1, ania-6a	1423622_a_at	NM_019937
Ccne1	Cyclin E1	1416492_at	NM_007633
Cnnm3	Cyclin M3, Acdp3	1420481_at	NM_001039551
Ccnl2	Cyclin L2, SB138, Ania-6b	1454149_a_at	NM_207678
Ccnh	Cyclin H	1418584_at	NM_023243
Ccnt2	Cyclin T2, CycT2	1427088_at	NM_028399
E2f1	E2F-1, E2f1	1431875_a_at	NM_007891
Mki67	Ki-67, Mki67	1426817_at	XM_001000692
Pcna	Pcna	1417947_at	NM_011045
Asymmetric cell division markers			
Notch3	Notch3	1421964_at NM_008716	
Dll4	Delta4, Dll4, delta-like 4	1421827_at	NM_019454
Dll1	Delta1, Dll1, delta-like 1	1419204_at	NM_007865
Numb	Numb, mnb, m-numb	1416891_at	NM_010949